

# DYNAMICAL MODEL OF THE MSG ATTITUDE

Oscar Luengo

*EUMETSAT (GMV consultant),  
Am Kavalleriesand, 31. D-64295 Darmstadt, Germany,  
E-mail: luengo@eumetsat.de*

## ABSTRACT

The Meteosat Second Generation (MSG) is a family of geostationary spin stabilised satellites, with an imaging instrument (SEVIRI) capable of providing measurements of stars, Earth horizon and Earth landmarks, apart from the images used for meteorological purposes. This instrument has a 20 kg mirror that rotates around an axis parallel to the S/C X axis (Z axis corresponds to the spin axis, X axis points out the satellite through the SEVIRI field of view and Y form the right-handed reference system). This rotation can be described as an initial stage in which the mirror is positioned in the starting point to obtain the meteorological data, a second stage in which the instrument is fixed (doing calibrations), and a final stage in which the meteorological images are taken. This movement (specially first and last stages) generates a variation in the inertia matrix of the satellite, resulting in nutation effects during the scanning and retracing phases. The present paper describes the dynamical modeling and the simulation of this effect, taking into account not only the inertia properties, but also the effect of anti-nutation measures provided by the design of the spacecraft (passive nutation dampers and a special profile in the positioning of the SEVIRI mirror).

## 1. FORMULATION OF THE DYNAMICS

The formulation used to describe the attitude dynamics is the well-known Euler's equations in its complete form, that is taking into account the variation of the inertia matrix with respect to the time. Then, the general equation that describes the MSG attitude can be written as:

$$\frac{dJ}{dt}\bar{\omega} + J\frac{d\bar{\omega}}{dt} = \bar{T} - \bar{\omega} \times J\bar{\omega} \quad (1)$$

Being  $J$  the inertia matrix,  $\bar{\omega}$  the rotation vector and  $\bar{T}$  the external torques. The time-dependant part of  $J$ , is going to complicate the formulation of the dynamical behaviour of the spacecraft.

## 2. CUSTOMISATION OF THE EQUATIONS TO THE MSG CASE

In order to use the operational data provided by the manufacturer, the main customisation of equation 1 is

the splitting of the inertia matrix in two: the spacecraft without the moving instrument, and the moving instrument itself.

The other important effect to be taken into account is the passive nutation damping placed in the spacecraft frame.

As external torque only the solar radiation will be taken into account.

### 2.1. Decomposition of the inertia matrix

As it has been mentioned, the approach taken in the current study is to distinguish between the SEVIRI, and the spacecraft-without-SEVIRI inertia. The manoeuvres are not considered, hence the latter one can be considered as constant. Moreover, the SEVIRI is rotating, so this rotation has to be added up when computing the angular momentum. Taking all this into account, the formulation of the corresponding differential equations can be written as follows:

$$\frac{dJ_{SEV}}{dt}(\bar{\omega} + \bar{h}) + (J_B + J_{SEV})\frac{d\bar{\omega}}{dt} + J_{SEV}\frac{d\bar{h}}{dt} = \bar{T} - \bar{\omega} \times ((J_B + J_{SEV})\bar{\omega} + J_{SEV}\bar{h}) \quad (2)$$

Where  $J_{SEV}$  is the SEVIRI inertia matrix,  $J_B$  is the S/C inertia matrix (w/o the SEVIRI instrument), and  $\bar{h}$  is the SEVIRI rotation.

And isolating the differential term  $\bar{\omega}$ :

$$\frac{d\bar{\omega}}{dt} = (J_B + J_{SEV})^{-1} \left[ \bar{T} - \bar{\omega} \times ((J_B + J_{SEV})\bar{\omega} + J_{SEV}\bar{h}) - J_{SEV}\frac{d\bar{h}}{dt} - \frac{dJ_{SEV}}{dt}(\bar{\omega} + \bar{h}) \right] \quad (3)$$

This is the form in which the equations are solved in the simulations.

#### 2.1.1. The SEVIRI inertia matrix (and derivatives)

Because the SEVIRI is moving continuously, and displaced from the theoretical centre of gravity of the spacecraft, the inertia matrix will be expressed in such a way as to be able to use homogeneous transformations. This way, the rotation/displacement of the instrument w.r.t. the spacecraft reference frame is applied through the use of a 4x4 transformation matrix. The

homogeneous inertia matrix is different from the standard one, although the mapping is quite straightforward. The general formulation of this matrix can be defined by:

$$\hat{J} = \begin{bmatrix} \frac{J_y + J_z - J_x}{2} & P_{xy} & P_{xz} & Mx_{CG} \\ P_{xy} & \frac{J_z + J_x - J_y}{2} & P_{yz} & My_{CG} \\ P_{xz} & P_{yz} & \frac{J_x + J_y - J_z}{2} & Mz_{CG} \\ Mx_{CG} & My_{CG} & Mz_{CG} & M \end{bmatrix} = \begin{bmatrix} \hat{J}_x & P_{xy} & P_{xz} & Mx_{CG} \\ P_{xy} & \hat{J}_y & P_{yz} & My_{CG} \\ P_{xz} & P_{yz} & \hat{J}_z & Mz_{CG} \\ Mx_{CG} & My_{CG} & Mz_{CG} & M \end{bmatrix} \quad (4)$$

Where  $J_i$  ( $i=x, y, z$ ) corresponds to the moments of inertia around the coordinate axis (as they appear in the typical inertia matrix),  $P_{ij}$  ( $i, j=x, y, z, i \neq j$ ) are the cross products,  $i_{CG}$  ( $i=x, y, z$ ) are the coordinates of the centre of gravity and  $M$  is the mass of the body.

Assuming that the initial matrix is given with reference to the principal axis of inertia, the matrix is given by:

$$\hat{I} = \begin{bmatrix} \hat{J}_x & 0 & 0 & 0 \\ 0 & \hat{J}_y & 0 & 0 \\ 0 & 0 & \hat{J}_z & 0 \\ 0 & 0 & 0 & M \end{bmatrix} \quad (5)$$

The mapping between the diagonal elements of both kinds of inertia matrices (standard and homogeneous) is:

$$\begin{aligned} J_x &= \hat{J}_y + \hat{J}_z \\ J_y &= \hat{J}_z + \hat{J}_x \\ J_z &= \hat{J}_x + \hat{J}_y \end{aligned} \quad (6)$$

If the matrix has to be expressed in a different reference frame, then the expression to be used is:

$$\hat{J}_{SEV}^B = T \cdot \hat{J}_{SEV}^{SEV} \cdot T^T \quad (7)$$

Where  $\hat{J}_{SEV}^B$  is the homogeneous inertia matrix of the SEVIRI instrument with reference to the body-fixed reference frame,  $\hat{J}_{SEV}^{SEV}$  is the homogeneous inertia matrix of the SEVIRI instrument with reference to the SEVIRI reference frame (subscripts refer to elements and superscripts refer to reference frames), and  $T$  is the homogeneous transformation matrix from SEVIRI to S/C body reference frame. In this case, this matrix is defined by:

$$T = \begin{bmatrix} \cos q & 0 & \sin q & p_x \\ 0 & 1 & 0 & p_y \\ -\sin q & 0 & \cos q & p_z \\ 0 & 0 & 0 & 1 \end{bmatrix} \quad (8)$$

Where  $q$  is the SEVIRI rotation angle, and  $p_i$  ( $i=x, y, z$ ) is the coordinates of the origin of the SEVIRI reference frame with reference to the S/C body reference frame.

For the SEVIRI, the values of  $p_x$ ,  $p_y$  and  $p_z$  can be defined as:

$$p_x = d_2 \sin q - d_3 \quad (9)$$

$$p_y = 0$$

$$p_z = d_1 + d_2 \cos q$$

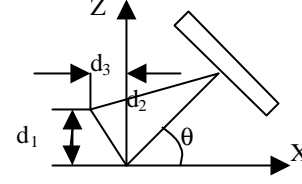


Fig. 1: SEVIRI position w.r.t. S/C

The resulting matrix, once the transformation is applied is:

$$\hat{J}_{SEV}^B = \begin{bmatrix} \hat{J}_x \cos^2 q + \hat{J}_y \sin^2 q + M(d_2 \sin q - d_3)^2 & 0 & \sin q \cos q (\hat{J}_z - \hat{J}_x) + M(d_1 + d_2 \cos q)(d_2 \sin q - d_3) & M(d_2 \sin q - d_3) \\ 0 & \hat{J}_y & 0 & 0 \\ \sin q \cos q (\hat{J}_z - \hat{J}_x) + M(d_1 + d_2 \cos q)(d_2 \sin q - d_3) & 0 & \hat{J}_z \sin^2 q + \hat{J}_y \cos^2 q + M(d_1 + d_2 \cos q)^2 & M(d_1 + d_2 \cos q) \\ M(d_2 \sin q - d_3) & 0 & M(d_1 + d_2 \cos q) & M \end{bmatrix} \quad (10)$$

Then, the standard inertia matrix of the SEVIRI instrument (applying the mapping between the homogeneous and standard inertias) is as follows:

$$J_{SEV}^B = \begin{bmatrix} J_x \sin^2 q + J_y \cos^2 q + M(d_1 + d_2 \cos q)^2 & 0 & \sin q \cos q (J_z - J_x) + M(d_1 + d_2 \cos q)(d_2 \sin q - d_3) \\ 0 & J_y & 0 \\ \sin q \cos q (J_z - J_x) + M(d_1 + d_2 \cos q)(d_2 \sin q - d_3) & 0 & J_z \sin^2 q + J_y \cos^2 q + M(d_1 + d_2 \cos q)^2 \\ J_x \sin^2 q + J_y \cos^2 q + M(d_1 + d_2 \cos q)^2 & 0 & M(d_1 + d_2 \cos q) & M \end{bmatrix} \quad (11)$$

The derivative with respect to time is:

$$\frac{dJ_{SEV}^B}{dt} = \begin{bmatrix} (J_x - J_y) \sin 2q - 2M(d_1 + d_2 \cos q) d_2 \sin q & 0 & \sin 2q (J_z - J_x) + M(d_2^2 \cos 2q + d_1 d_2 \sin q + d_1 d_2 \cos q) \\ 0 & -2M(d_1 d_2 \sin q + d_1 d_2 \cos q) & 0 \\ \sin 2q (J_z - J_x) + M(d_2^2 \cos 2q + d_1 d_2 \sin q + d_1 d_2 \cos q) & 0 & (J_x - J_y) \sin 2q + 2M(d_1 \sin q - d_3) d_2 \cos q \end{bmatrix} \frac{dq}{dt} \quad (12)$$

## 2.2. Nutation Damping

The MSG S/C has two types of nutation damping:

- Active Nutation Damping (AND)
- Passive Nutation Damping (PND)

The first one corresponds to an active control performed by the on-board AOCs and based in measurements taken from the accelerometers. It is only used during the LEOP.

The second one is the one to be modelled. The S/C has two passive nutation dampers, which contains a special fluid that due to the effect of movement and dissipation provides a mean to achieve the dumping of the nutation. Two different models have been developed to describe this effect.

### 2.2.1. Simple model

The first one was a very simple model of a viscous angular damper mounted on the y-axis. The viscous torque generated by this model is described in eq. (13)

$$T_{PND} = \begin{bmatrix} 0 & 0 & 0 \\ 0 & B & 0 \\ 0 & 0 & 0 \end{bmatrix} \vec{\omega} \quad (13)$$

Where  $B$  is the viscous damping, and  $\vec{\omega}$  is the angular velocity vector.

The resulting Euler equation is as follows:

$$\frac{d\vec{\omega}}{dt} = (J_B + J_{SEV})^{-1} \left[ \vec{T} - \vec{\omega} \times ((J_B + J_{SEV})\vec{\omega} + J_{SEV}\vec{h}) - J_{SEV} \frac{d\vec{h}}{dt} - \frac{dJ_{SEV}}{dt}(\vec{\omega} + \vec{h}) + T_{PND} \right] \quad (14)$$

### 2.2.2. Not so-simple model

The second model corresponds to an equivalence of the physics of the PND with a spring-mass system. This is more accurate than the model presented in the previous section, although it is much more computationally expensive since it requires 7 state variables (as will be showed later). The typical formulation is:

$$M \frac{d^2 q}{dt^2} = F - Kq - B \frac{dq}{dt} \quad (15)$$

Where  $M$  is the mass of the system,  $q$  is the distance measure along the line where the spring-mass is placed,  $F$  is the force applied,  $K$  is the characteristic constant of the spring and  $B$  is the viscous force.

In order to allow the proper use of standard mathematical packages, the formulation of the spring-mass system has to be done in terms of state variables (in this case, position and velocity):

$$\frac{d}{dt} \begin{bmatrix} u \\ v \end{bmatrix} = \begin{bmatrix} 0 & 1 \\ -\frac{K}{M} & -\frac{B}{M} \end{bmatrix} \begin{bmatrix} u \\ v \end{bmatrix} + \begin{bmatrix} 0 \\ \frac{F}{M} \end{bmatrix} \quad (16)$$

$u = q$   
 $v = \frac{dq}{dt}$

This formulation is used for both dampers, so two systems of these will be used. This explains the increase from three state variables (the three components of the angular velocity) to seven.

The new state vector  $\Gamma$  is defined by the following variables:

$$\Gamma = \begin{bmatrix} w_x \\ w_y \\ w_z \\ q_1 \\ vq_1 \\ q_2 \\ vq_2 \end{bmatrix} \quad (17)$$

Where  $q_1$  is the linear displacement of the first PND,  $vq_1$  the linear speed of the first PND,  $q_2$  is the linear

displacement of the second PND,  $vq_2$  the linear speed of the second PND.

Let's assume that the variation of the inertia of these dampers are negligible (this will imply a simplification in the matrix that multiplies the derivative term in the left-hand side in the equation of the dynamics). The structure of the equations is as follows:

$$\Lambda \frac{d}{dt} \Gamma = \begin{bmatrix} \vec{T} - \vec{\omega} \times ((J_B + J_{SEV} + J_{PND1} + J_{PND2})\vec{\omega} + J_{SEV}\vec{h}) - J_{SEV} \frac{d\vec{h}}{dt} - \frac{dJ_{SEV}}{dt}(\vec{\omega} + \vec{h}) \\ \frac{0}{M_1} \frac{1}{M_1} \begin{bmatrix} q_1 \\ vq_1 \end{bmatrix} + \begin{bmatrix} 0 \\ \vec{\omega} \times (\vec{\omega} \times \vec{r}_1) \end{bmatrix} \vec{h}_1 \\ \frac{0}{M_2} \frac{1}{M_2} \begin{bmatrix} q_2 \\ vq_2 \end{bmatrix} + \begin{bmatrix} 0 \\ \vec{\omega} \times (\vec{\omega} \times \vec{r}_2) \end{bmatrix} \vec{h}_2 \end{bmatrix} \quad (18)$$

Remind only that  $\vec{u}$  is the alignment of the damper, and  $\vec{r}$  is the position of the mass.

The first three rows of the right-hand side are the right-hand side of the Euler equation (see eq. 3), with the only difference that the inertia of the PNDs has to be added. The following two rows corresponds to the dynamics of the first PND, and the last two ones to the second PND. The matrix  $\Lambda$  can be called pseudo-inertia matrix, since it contains the information of the inertia of the system, but also the coupling between this inertia and the dynamics of the two dampers. The matrix has a dimension of 7x7. Taking in to account that the problem is quite sensitive to these dimensions (because of the short steps to be taken during the numerical integration) let's take a look at its structure:

$$\Lambda = \begin{bmatrix} & & & & & & 0 & 0 & 0 & 0 \\ & & & & & & 0 & 0 & 0 & 0 \\ & & & & & & 0 & 0 & 0 & 0 \\ & & & & & & 1 & 0 & 0 & 0 \\ & & & & & & 0 & 1 & 0 & 0 \\ & & & & & & 0 & 0 & 1 & 0 \\ & & & & & & 0 & 0 & 0 & 1 \end{bmatrix} = \begin{bmatrix} A \\ C \\ D \end{bmatrix} \quad (19)$$

Where  $\cos \mathbf{a}$ ,  $\cos \mathbf{b}$  and  $\cos \mathbf{g}$  are the cosines that define the alignment of the dampers (i.e. the components of  $\vec{u}$ ), and  $r_{ij}$  corresponds to the  $j$  component of dumper  $i$ . The matrix is divided in 4 boxes, and its structure (along with the existence of the identity matrix in the fourth box of the diagonal) allows obtaining the inverse of a 7x7 matrix by the inversion of a 3x3 matrix and the multiplication of a 4x3 matrix and a 3x3 matrix:

$$\Lambda^{-1} = \begin{bmatrix} J_{TOT}^{-1} & 0 \\ -CJ_{TOT}^{-1} & I \end{bmatrix} \quad (20)$$

## 3. SIMULATIONS

### 3.1. Inputs

The second step (once the model is defined), is setting-up the inputs to the system. For the present work, and strictly speaking, there is just one input to the system,

which is the solar torque. There is also another source of “perturbation”, which is the movement of the SEVIRI instrument. It causes the inertia matrix to vary, and hence modify rotations around the three axes. For this reason, the angle of the instrument will be taken into account, and considered as input in the present study. The angle shows the typical cycle in the scanning process, which is:

- Retracing: coming back to the initial position to start the scanning.
- Calibration: short period in which the mirror is calibrated against a black body.
- Scanning: the image is obtained.

The shape of the angle profile can be seen in the following figure, and although it varies depending on the season, the shape is typically the same:

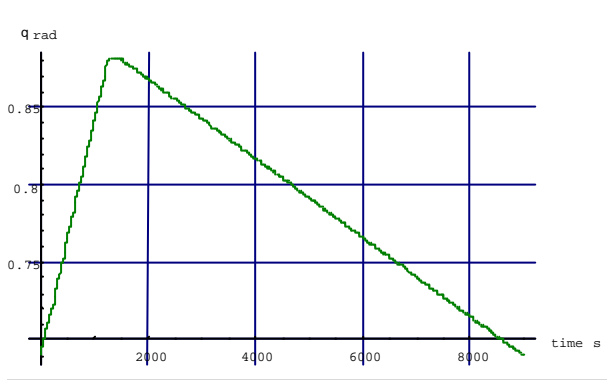


Fig. 2: Angle profile of SEVIRI

Although it looks a straight line, the motor used to move the mirror is a stepper one, so if a more detailed view of the profile is taken, the real shape is:

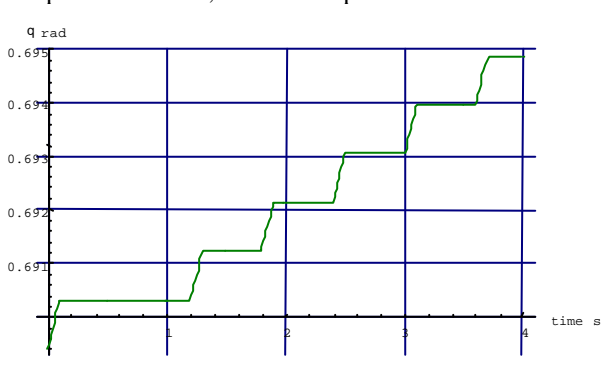


Fig. 3: First 4 seconds of the SEVIRI angle

The initial rise is modelled as an S-curve (which is the typical one for servoing electric motors), and it lasts for 5% of 1-revolution time. It can also be seen that after the first step, there is a revolution with no movement at all (from now on defined as waiting step, being the nominal a 1-waiting step). The reason for that is to minimise the nutation produced by the SEVIRI movement taking advantage of the nutation fade-out due to the lack of input. There is also another of these

“blank” steps, just one step before reaching the target position.

The input will consist in two consecutive cycles as the one described, mainly to avoid the transient terms in the first one, and see the steady-state effects in the second one.

### 3.2. Results

The following sections will show figures with three different plots, each one corresponding to the x, y and z components respectively of the satellite rotation vector in spacecraft reference frame (in rad/s).

#### 3.2.1. Simple model of damper. Nominal profile

Fig. 4 shows the results after simulating 2 nominal cycles of the SEVIRI instrument.

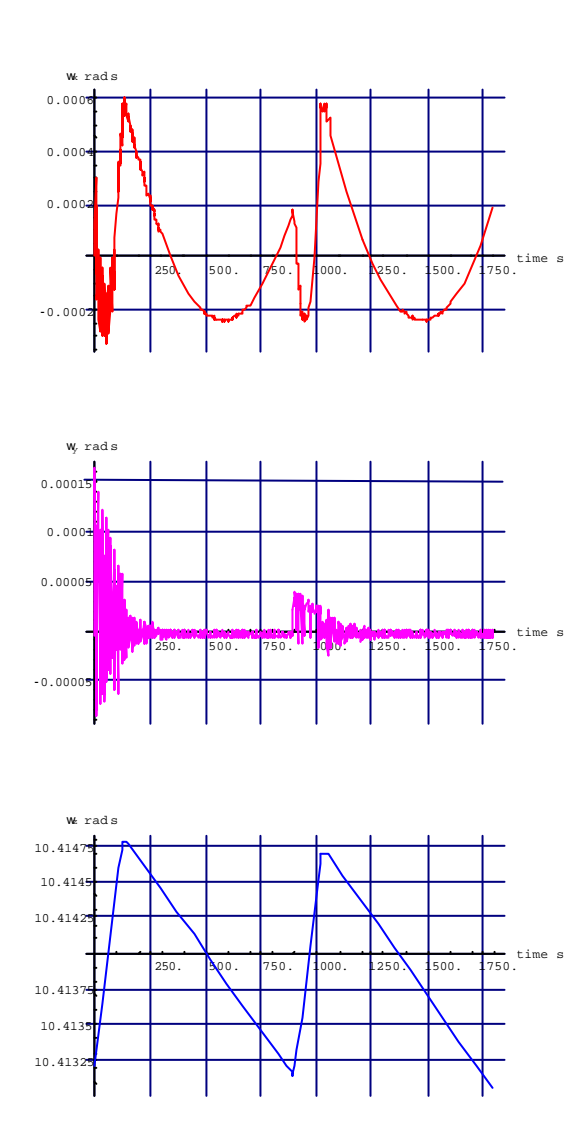


Fig. 4: Results of the simulation (simple damper, nominal profile).

The effect of the nutation is clearly seen around 1000 seconds in the middle graph, with maximum amplitude of less than  $5 \times 10^{-4}$  rad/s.

### 3.2.2. Simple model of damper. No waiting steps

Fig. 5 shows the results of the simulation.

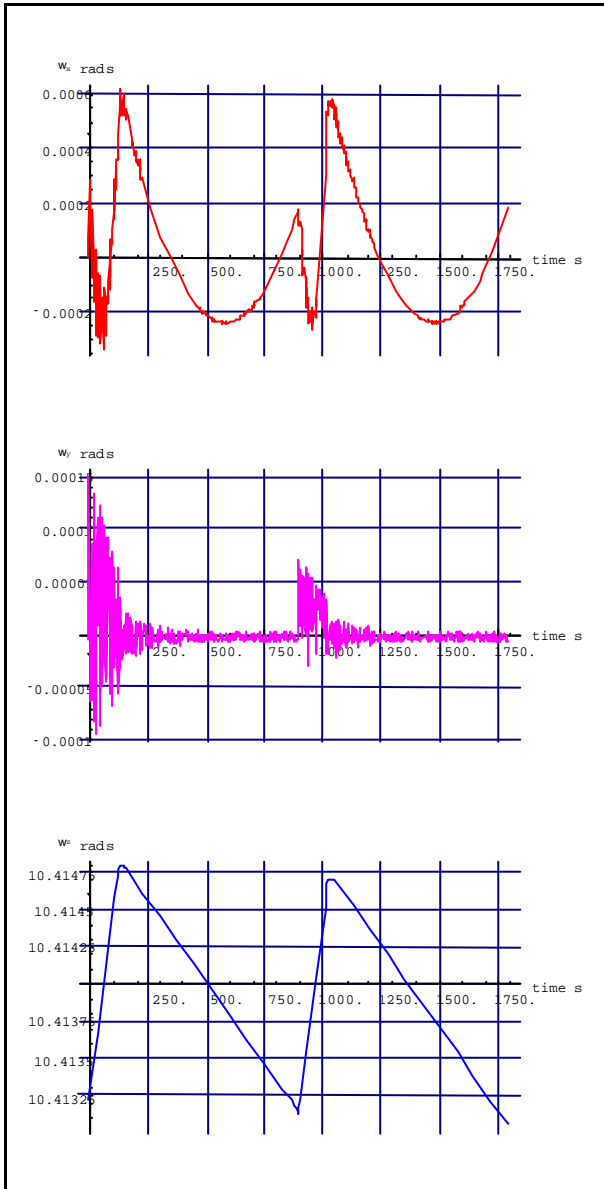


Fig. 5: Results of the simulation (simple damper, no waiting step)

The most remarkable aspect of the graph is the increment in the amplitude of the nutation (during the transient mode) about 50 % with respect to the results shown in Fig. 4 (which confirms the suitability of the nutation damping approach).

### 3.2.3. Simple model of damper. 2-waiting steps

Fig. 6 shows the results of the simulation.

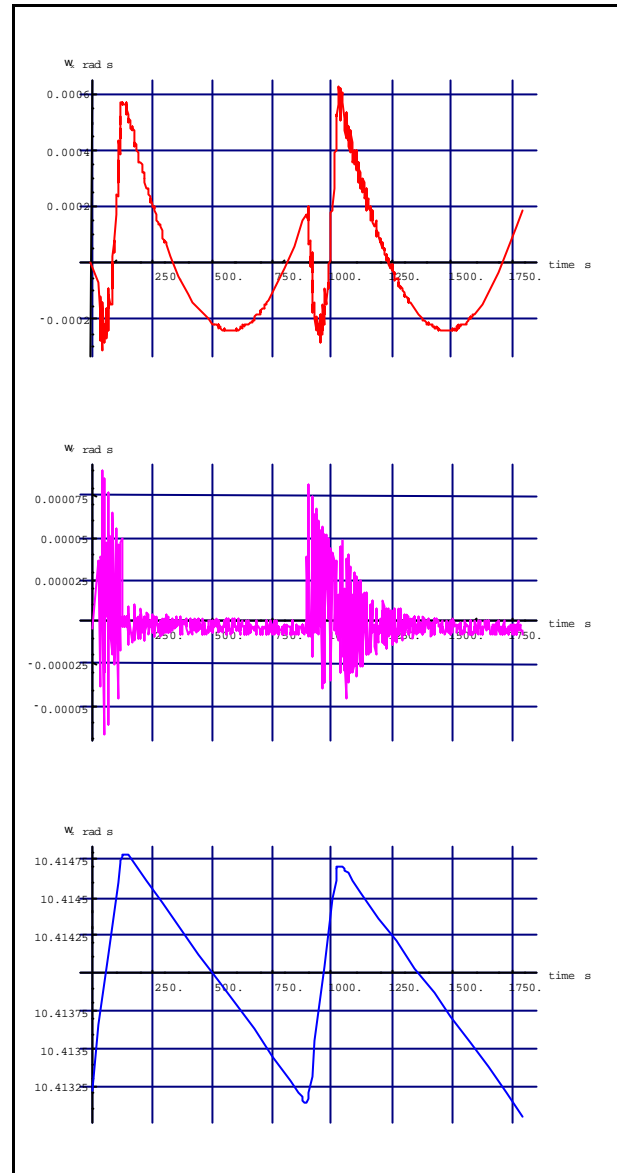


Fig. 6: Results of the simulation (simple damper, 2-waiting steps)

This is the worst case among the ones showed in the present study. It can be explained by the starting of a new nutation cycle (after the stop) on a state that corresponds to a maximum in amplitude of the nutation fade-out.

### 3.2.4. Simple model of damper. 6-waiting steps.

Fig. 7 shows the results of the simulation.

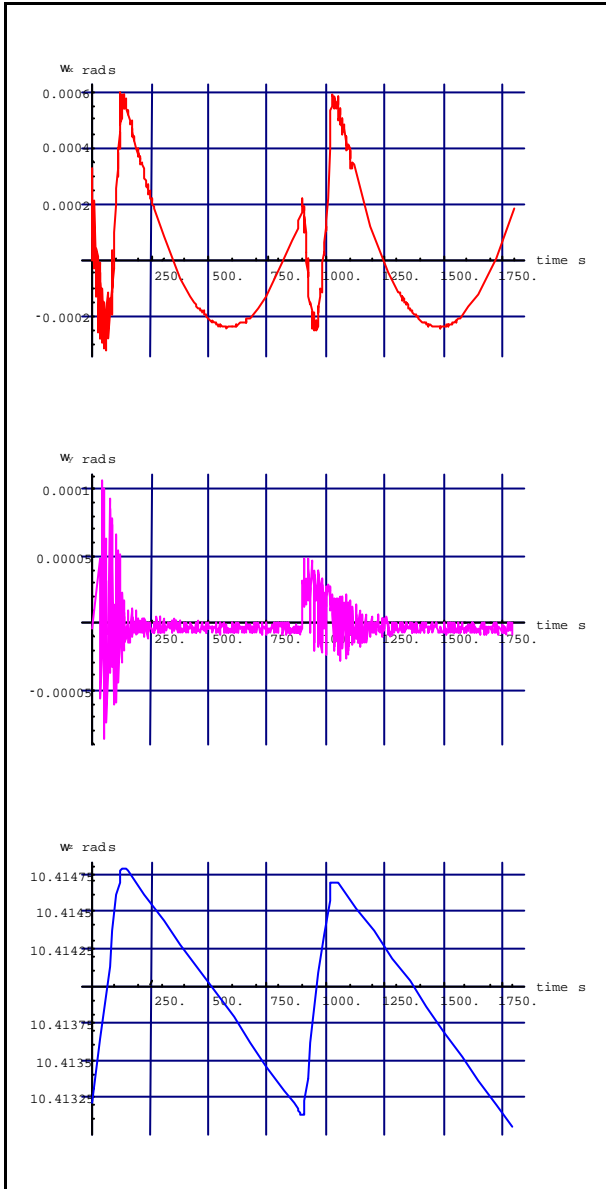


Fig. 7: Results of the simulation (simple damper, 6-waiting steps)

The peak values observed are pretty similar to the ones observed in the 1-cycle stop. This time the SEVIRI rotation is stopped almost one nutation cycle, which implies a quite long progress in the nutation fade-out. The reason for higher mean-peak values can be found in a non-optimal start of the new nutation cycle.

### 3.2.5. Not so simple model of dumper.

The implementation of the more accurate model of the dumper into the simulation does not provide much more information to the one obtained with the simpler one. In fact the maximum values and timing are equivalent. For standard mathematical packages like MatLab, SciLab or Matlab it implies simulations of more than 2 hours, which does not justify its use since the characteristic results are almost the same.

## 4. CONCLUSIONS

It has been presented a formulation of the attitude dynamics of the MSG satellites taking into account the variation of the inertia due to the movements of the SEVIRI instrument. The PND implemented by the manufacturer has been modelled as well. The results showed in the graphs correspond quite exactly to the reality that can be sensed through telemetry readings, which confirms the correctness of the model. The simulations of the model with the spring-mass dampers have shown that the increase in accuracy does not justify the high amount of time spent in the simulations.

The implementation of this model using a standard programming language such as Fortran90 or C++, would increase the performance of the model and ease its use for off-line analysis of the attitude behaviour of this operational family of spacecrafts.

## 5. ACKNOWLEDGEMENTS

The author wishes to thank to the people of the Flight Dynamics Group at Eumetsat for his support during the realisation of this paper.